Spin transport through a junction entirely consisting of molecules from first principles

Huan Wang,[1] Jia Zhou,[1] Xiaojie Liu,[1,a)] Chengbao Yao,[1] Hua Li,[1] Li Niu,[1] Yin Wang,[2] and Haitao Yin[1,a)]
[1]*Key Laboratory for Photonic and Electronic Bandgap Materials of Ministry of Education, School of Physics and Electronic Engineering, Harbin Normal University, Harbin 150025, China*
[2]*Department of Physics and Shenzhen Institute of Research and Innovation, The University of Hong Kong, Pokfulam Road, Hong Kong, China*

(Received 2 May 2017; accepted 18 October 2017; published online 27 October 2017)

Using first-principles calculations based on density functional theory combined with the nonequilibrium Green's function formalism, we studied the spin transport through a single molecular junction which consists of a single 1,4-benzenedithiolate (BDT) molecule and two ferromagnetic electrodes $[(Ge_5)Fe]_\infty$. A large magnetoresistance ratio (MR) of 21100% was found in the $[(Ge_5)Fe]_\infty$-BDT-$[(Ge_5)Fe]_\infty$ molecular junction at small bias voltage, and the MR value decreased with the increase in the applied bias voltage. For the parallel magnetization configuration, the molecular junction showed outstanding spin injection effects. Negative differential resistance was observed for the antiparallel magnetization configuration. Spin dependent transmission spectra at different bias voltages were used to explain the calculated results. *Published by AIP Publishing.*
https://doi.org/10.1063/1.5009744

Magnetic tunnel junctions (MTJs) exhibiting a high magnetoresistance (MR) have extremely important applications in magnetic random access memory (MRAM), magnetic sensors, and magnetic read heads. Generally, a traditional MTJ consists of two ferromagnetic layers separated by a nonmagnetic insulating layer, such as Al_2O_3 (Ref. 1) and MgO.[2,3] In the past few years, a considerable amount of effort has been made to improve the tunnel magnetoresistance (TMR) value. As we know, factors such as the barrier materials, electrodes, and their interfaces have important effects on the TMR value. This fact makes it more complicated for the quantitative description of the transport characteristics of MTJs. However, it on the other hand dramatically broadens the possibilities for altering the properties of MTJs. In particular, by modifying the electronic properties of electrodes, it is possible to engineer MTJs with properties desirable for device applications. In this context, for example, MTJs consisting of a MgO insulating barrier sandwiched between two Fe,[2] CoFeB,[4] or even Co-based Heusler alloy[5,6] electrodes were fabricated to get a high TMR value.

Molecules, especially, organic molecules, have the advantage of weak spin-orbit and hyperfine interactions, which preserve spin-coherence over time and distance much longer than that in conventional metals or semiconductors.[7,8] Such features make organic materials suitable for spin injection and transport.[9–11] Notice that the ferromagnetic electrodes used in molecular spintronics devices are conventional inorganic bulk materials, while the organic material is only used as a spacer. Hence, one of the standing challenges in molecular spintronics is to use molecular-based ferromagnetic materials as spin injecting electrodes. Recently, types of sandwich complexes, $(Ge_5)_2Fe$, were synthesized.[12] Experimental results have shown that they are highly stable. So far, longer chains of [(Ge5)Fe] have not been made experimentally. Recently, the metallic and ferromagnetic one-dimensional sandwich polymer $[(Ge_5)Fe]_\infty$,[13] whose crystal structure and electronic structure are shown in Figs. 1(a)–1(c), has been predicted from the first-principles method. The magnetic moment of the $[(Ge_5)Fe]_\infty$ sandwich polymer is predicted to be 2.863 μ_B. Compared with the ferromagnetic metals Fe, Co, and Ni, which are often considered for use as the electrode in MTJs, with magnetic moments of 2.13μ_B, 1.52μ_B, and 0.57μ_B,[14] respectively, the $[(Ge_5)Fe]_\infty$ sandwich polymer could be a potential alternative candidate for electrode use and could serve to enhance the spin injection efficiency (SIE) and MR value in one-dimensional molecular spintronics devices.

While contributions of diverse molecules and electrodes on MR and SIE have remained the focus of active theoretical research in recent years, few studies address the role played by the one-dimensional magnetic electrodes in molecular devices. To this end, we investigated the spin-polarized transport of one-dimensional magnetic molecular junction in which a 1,4-benzenedithiolate (BDT) molecule is contacted with two ferromagnetic polymer electrodes, $[(Ge_5)Fe]_\infty$, as schematically shown in Fig. 1(d). In contrast to previous works, here we replaced the usual bulk ferromagnetic electrodes with the $[(Ge_5)Fe]_\infty$ polymer and investigated the possibility of increasing the MR and SIE. The calculated results suggest that in this one-dimensional molecular magnetic junction, the highest MR ratio that can be reached is 21 100%. Compared with the results of BDT connected with bulk magnetic lead, this improvement of MR ratio is significant.

The molecule device is divided into three regions, left electrode, right electrode, and center region [see Fig. 1(d)]. In screening approximation,[15] the left and right electrodes composed of a $(Ge_5)Fe$ sandwich polymer are semi-infinite, which guarantees that in the electrode regions, the potential

a)Authors to whom correspondence should be addressed: redlxj@163.com and wlyht@126.com

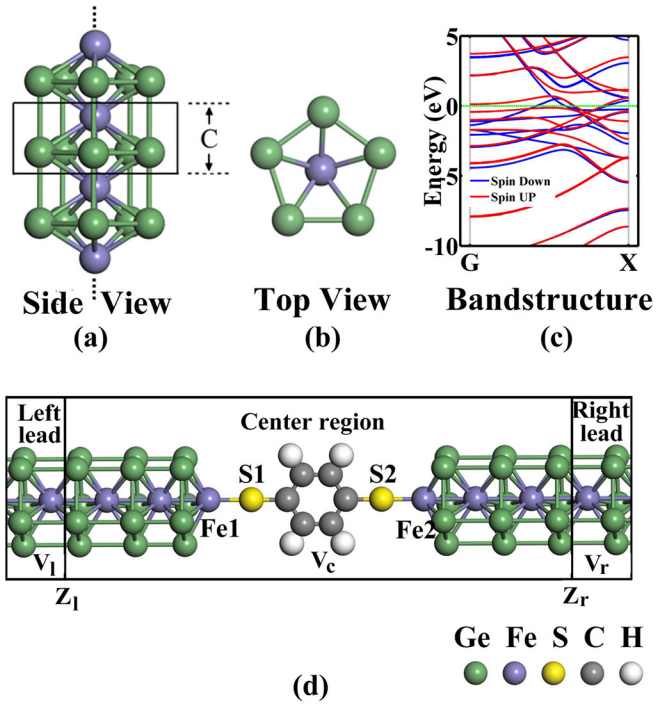

FIG. 1. Structure model of the molecular devices. (a) Side view and (b) top view of the structure of $[(Ge_5)Fe]_\infty$ sandwich polymer. The enclosed region in part indicates the unit cell of the polymer, and the lattice constant C is 2.71 Å. (c) Band structure of $[(Ge_5)Fe]_\infty$ sandwich polymer. (d) Schematic plot of a single 1,4-benzenedithiolate molecule (BDT) attached to $[(Ge_5)Fe]_\infty$ electrodes. The buffer layer is thick enough so that the Hartree potentials satisfy the natural boundary condition, that is, $V_c(r)|_{Z_l} = V_l(r)|_{Z_l}$ and $V_c(r)|_{Z_r} = V_l(r)|_{Z_r}$, where the planes Z_l and Z_r are the left and right limits of the center region. $V_c(r)$, $V_l(r)$, and $V_r(r)$ are the Hartree potentials of the center region, the left lead, and right lead, respectively.

is bulk like and the electron motion is governed by a bulk Hamiltonian. The center region is composed of BDT and enough buffer layers. Five unit cells of both electrodes were used as the buffer layers in the center region to screen the Hartree potential and determine the boundary conditions of the center region through the corresponding electrode.[15] The difference in the voltages of the two electrodes sets up a steady state electron flow from one electrode to another.

The structures of the $[(Ge_5)Fe]_\infty$ polymer and single molecule BDT are first optimized independently with VASP,[16] employing the local density approximation (LDA) for the exchange-correlation functional, and then the whole structure is further fully relaxed until the force on each atom is less than 0.05 eV/Å. The spin transport through the devices was investigated by the method of density functional theory (DFT) combined with the nonequilibrium Green's function (NEGF), as implemented in the Nanodcal.[15] A linear combination of atomic orbitals (LCAO) was employed. The valence electronic orbitals of the system were described using the double-zeta polarized (DZP) basis set, and the atomic core was defined by the standard nonlocal norm-conserving pseudopotential.[17] The exchange-correlation was taken into account at the LDA level.

We calculated the spin-dependent transmission coefficients from Green's functions as

$$T_\sigma \equiv Tr\left[\mathrm{Im}\left(\Sigma_L^r\right)G^r\mathrm{Im}\left(\Sigma_R^r\right)G^a\right], \quad (1)$$

where $\sigma \equiv \uparrow, \downarrow$ is the spin index; $\Sigma_{L/R}^r$ are the retarded self-energy of the left (right) leads, which reflect the coupling between the central scattering region and the leads; and $G^{r(a)}$ are the retarded (advanced) Green's function matrices in spin and orbital space.

The spin-dependent current was further obtained using the Landauer–Büttiker formula[18,19]

$$I_\sigma(V) = \frac{e}{h}\int_{\mu_L}^{\mu_R} dET_\sigma(E, V_L, V_R)[f_L(E, \mu_L) - f_R(E, \mu_R)], \quad (2)$$

where $\mu_L(\mu_R)$ are the electrochemical potentials of the left and right leads and $f_L(f_R)$ are the Fermi distribution functions of the left and right leads. $V_{L/R}$ are the bias voltages applied on the left and right leads. The transmission coefficient $T_\sigma(E, V_L, V_R)$ is a function of the energy E, V_L, and V_R. The total charge current is $I = I_\uparrow + I_\downarrow$. From the values of currents at different voltages, the MR ratio can be calculated by the following formula:[20,21]

$$\mathrm{MR} = \frac{R_{APC} - R_{PC}}{R_{PC}} = \frac{I_{PC} - I_{APC}}{I_{APC}}, \quad (3)$$

where R_{PC} and R_{APC} are the resistances, and I_{PC} and I_{APC} are the total charge currents in the parallel magnetization configuration (PC) and the antiparallel magnetization configuration (APC), respectively. Another important quantity is the SIE, which is defined as $\eta = |I_\uparrow - I_\downarrow|/|I_\uparrow + I_\downarrow|$. At zero bias when all currents vanish, we use the transmission coefficient at the Fermi level instead of the current I to calculate the MR and SIE values, namely, $\mathrm{MR} = (T_{\mathrm{PC}}(\mathrm{E_F}) - T_{\mathrm{APC}}(\mathrm{E_F}))/T_{\mathrm{APC}}(\mathrm{E_F})$ and $\eta = |T_\uparrow(\mathrm{E_F}) - T_\downarrow(\mathrm{E_F})|/(T_\uparrow(\mathrm{E_F}) + T_\downarrow(\mathrm{E_F}))$, which can approximately reflect the transport properties of the molecular junction at very small bias.

When a bias V is applied between the two electrodes, we set $V_L = V/2$ and $V_R = -V/2$ in our calculation. Figures 2(a) and 2(b) present the I-V characteristics for PC and APC, respectively. The characteristic of the spin currents is different from the case of oxide tunnel barriers such as MgO,[2,3] and the π orbitals in BDT provide a good transport channel leading to metallic I-V curves. The spin currents are nonlinear functions of the applied bias voltages, and their values are a few thousands of nA for PC at large bias voltage range. For the small bias voltages (less than 0.6 V), the currents I increase with the increase in the bias voltages from zero. The currents reach their maximums at about 0.8 V for PC and 0.7 V for APC. After that, the currents drop with increasing bias and give rise to the phenomenon of negative deferential resistance (NDR).

As can be seen in Fig. 2(c), the MR ratio reaches a maximum of about 21 100% in the equilibrium state. Up to now, there has been a lack of experimental results regarding the MR of BDT connected to $[(Ge_5)Fe]_\infty$ leads. We compared our calculated results with the same molecule connected to other magnetic leads. Quantitatively, previous calculations on Ni/BDT/Ni junctions yielded widely different MR values ranging from 27% to 5282%,[11,22,23] and on Mn/BDT/Mn junctions, they yielded MR values of 340%.[22] Experimentally, the individual Ni/BDT/Ni junctions have been fabricated with MR values from 30% to 150%.[24,25] In this entire molecular junction, the

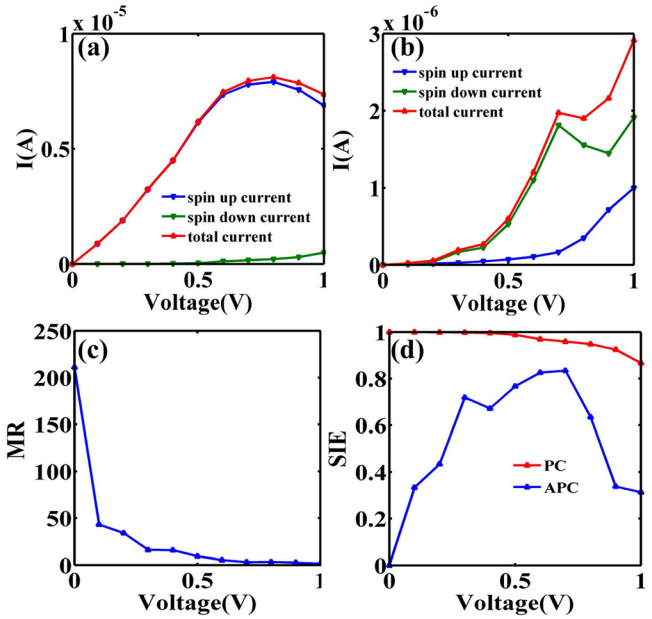

FIG. 2. Spin dependent currents versus bias voltage in (a) PC and (b) APC setup of the leads' magnetization. (c) MR and (d) spin-injection efficiency (SIE) versus the bias voltage, respectively.

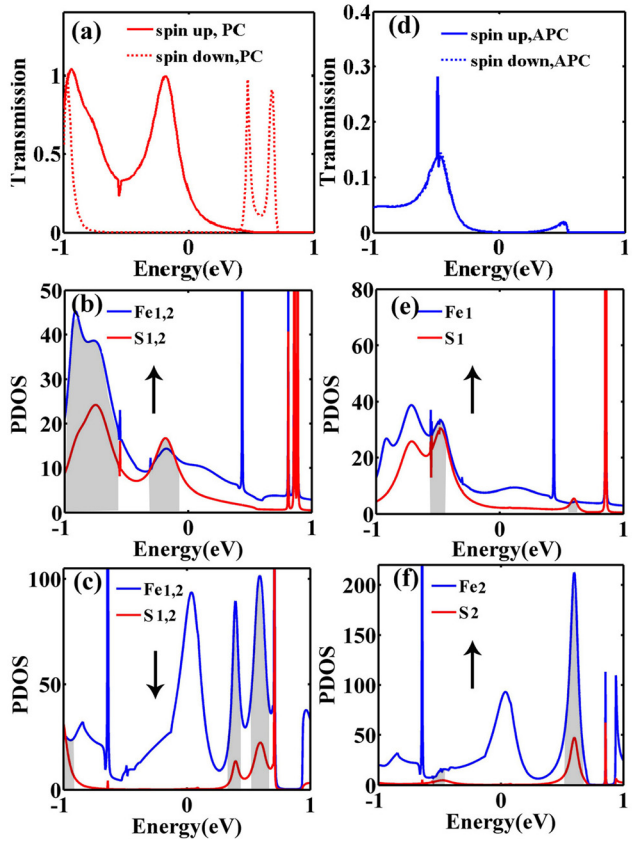

FIG. 3. Transmission coefficients and PDOS versus energy E in PC and APC setups at equilibrium. E = 0 is the Fermi energy of the leads. (a) Transmission and (b) PDOS of the spin up electron on Fe1 and S1 atoms. (c) PDOS of the spin down electron on Fe1 and S1 atoms in PC, red solid: $T_\uparrow$ and red dashed: $T_\downarrow$. (d) Transmission and PDOS of the spin up electron on (e) Fe1, S1 atoms and (f) Fe2, S2 atoms in APC, blue solid: $T_\uparrow$ and red dashed: $T_\uparrow$ with $T_\uparrow$=$T_\downarrow$. The shaded areas denote the overlap regions of PDOS which have contribution to the transmission.

improvement of the MR ratio is significant. With increasing applied voltage, the calculated MR is reduced gradually from the maximum to 153% eventually, at about 1 V. Such behavior is similar to that of a Ni-BDT-Ni junction[11] and conventional magnetic tunnel junctions.[26]

We also plot the SIE according to the spin currents at different voltages [see Fig. 2(d)]. The obvious features can be found: the SIE reaches about 100% for PC and then declines gradually with the increase in the voltage. The values and trend of SIE are the same as those of the BDT connected to Cobalt electrodes.[27] For APC, SIE starts from zero and increases to a maximum of about 83%, after which it decreases to 31%, at the bias voltage of 1 V.

The above characteristics of MR and SIE can be understood from the transmission spectrum through the molecular junction. Figures 3(a) and 3(d) plot the transmission coefficient T_σ as a function of energy E at zero bias in the PC and APC, respectively. For PC, at the Fermi energy, the $T_\uparrow$ curve is dominated by a wide resonance feature and $T_\downarrow$ is about zero. The spin up component transmission is much larger than that of the spin down component, showing an excellent spin injection effect at equilibrium. Note that for APC, the transmission spectra of spin down and spin up electrons overlap, which means $T_\downarrow$=$T_\uparrow$ for the entire energy range, due to the symmetry of the $[(Ge_5)Fe]_\infty$-BDT-$[(Ge_5)Fe]_\infty$ device. So it produces a zero SIE. Moreover, the total value of $T_\downarrow$+$T_\uparrow$ in PC is three orders of magnitude higher than that in APC, which leads to the extremely large values of MR at zero bias.

In order to explain the spin resolved transport properties, the projected densities of states (PDOS) of the junction have also been calculated. The PDOS are projected on the left Fe and S atoms [labeled Fe1 and S1 in Fig. 1(d)] and the right Fe and S atoms [labeled Fe2 and S2 in Fig. 1(d)] at the interfaces in PC and APC, respectively. Figure 3(b) shows the PDOS of the Fe1 and S1 atoms for PC at spin up states, and it can be observed that there exist three PDOS overlapping regions for the Fe1 and S1 atoms. In comparison with the transmission spectra at zero bias, the state overlapping regions correspond well to the transmission peaks. Note that the peak of transmission at about 0.8 eV is very small (being of the order of 10^{-3}), and it almost cannot be seen. The above states give rise to the broad transmission features near the Fermi energy. They allow spin up electrons to transmit efficiently through the metal-molecule interface and so give rise to a moderately strong transmission dominating the current in the experimentally accessible moderate bias regime. Figure 3(c) shows the PDOS of spin down states of the Fe1 and S1 atoms for PC, and the strong hybridization of the electrodes and the molecule in energy regions −1 eV, 0.47 eV, and 0.66 eV cause three transmission peaks. In general, the difference between hybrid states of spin up and spin down electrons gives rise to strongly spin dependent transport characteristics. In APC, the PDOS of the Fe1, Fe2, S1, and S2 atoms are shown only for spin up (the PDOS of Fe1, Fe2, S1, and S2 atoms for spin down are the same as the PDOS of Fe2, Fe1, S2, and S1 for spin up, respectively). The transmission spectra are dominated by both an overlap of states of the left Fe, S and the right Fe, S. As a result, there

are only two peaks at about −0.5 eV and 0.6 eV in the energy range of −1 eV–1 eV.

The above spin dependent properties originate from a degree of spin-resolved electronic hybridization when the nonmagnetic molecule is contacted by the ferromagnetic electrode. Indeed, the features of the PDOS and transmission coefficients are totally consistent with each other. We can further understand intuitively the voltage dependence of the spin current by analyzing the transmission coefficient at different bias voltages. Applying a bias voltage, the currents are closely related to the transmission coefficients lying between μ_L and μ_R according to the formula (2). As shown in Fig. 4, for PC, the spin-up transmission has a broad peak situated at about E = −0.2 eV [labeled by red "A" in Fig. 4(a)], and the spin-down transmission has a sharp peak located at about E = 0.4 eV [labeled by red "B" in Fig. 4(a)] at a bias of 0.2 V. With a further increase in bias voltages, the right tail of the "A" peak of the spin-up transmission enters the bias window, which leads to the increase in the spin-up current. The "B" peak of the spin-down channel does not contribute to the current at relatively small voltages. Accordingly, the spin-down current maintains zero approximately. The above characteristics of spin dependent transmission can result in the perfect SIE in the small voltage range. When the larger bias (>0.6 V) is applied, the spin-down current will be increased due to the peak labeled by red "B" in the spin-down channel when it enters the bias window and contributes to the current. The enhancing spin down current leads to the degradation of SIE. For the APC situation, the bias breaks the geometric symmetry and the spin-down channel gives larger contribution than the spin-up channel in the bias window, which makes $I\downarrow > I\uparrow$. The spin down current is mainly contributed to by the peak labeled by blue "D′" at a bias of 0.2 V. When the bias voltage is increased further, the peaks labeled by "B′" and "C′" of $T_\downarrow$ and the right tail of "A′" peak of $T_\uparrow$ entering the bias window and the increase in the peak labeled by "D′" of $T_\downarrow$ lead to the increase in the total currents of APC. Therefore, the increased APC current gives rise to the reduction of MR gradually. In addition, the integral value of the spin-down transmission coefficient at 0.8 V is found to be slightly smaller than that at 0.7 V and 0.9 V. That is why the current value decreased as the bias voltage increased from 0.7 V to 0.8 V and the NDR appeared in this voltage region.

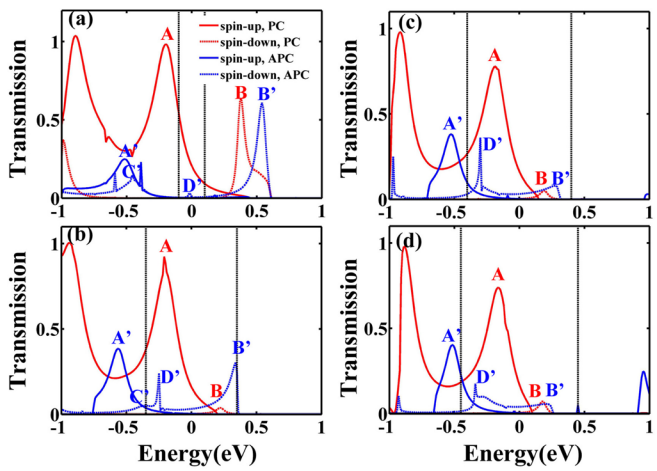

FIG. 4. Transmission coefficients versus energy E at different bias voltages. (a) 0.2 V; (b) 0.7 V; (c) 0.8 V; and (d) 0.9 V. Red solid: $T_\uparrow$ and red dashed: $T_\downarrow$ in PC; blue solid: $T_\uparrow$ and blue dashed: $T_\downarrow$ in APC setup, respectively. The two black vertical dashed lines represent the bias window in each panel.

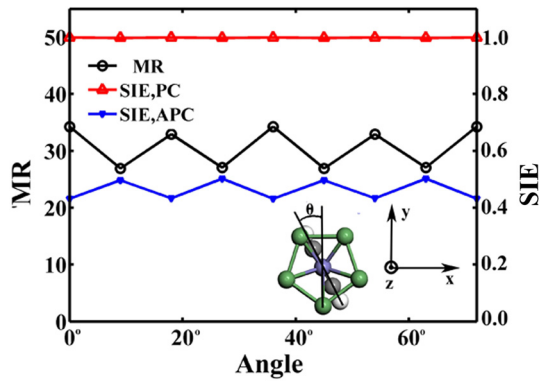

FIG. 5. MR and SIE versus the orientations of BDT between the two electrodes at $V = 0.2$ V. Inset: schematic representation of the tilting angles between the backbone of BDT and the yz plane. The angle θ is the tilting angle.

Finally, considering that the single BDT molecule has different orientations between the two electrodes, we further investigated the influence of those orientations on the spin-dependent transport through the devices. In our simulation, the positions of the electrodes and the distance between the two electrodes were fixed while the central molecule was rotated on the z axis (the connection between the Fe1 and Fe2 is set to the z axis). The angle θ is the tilting angle formed by the BDT molecular plane and the yz plane, which is illustrated in the inset of Fig. 5. Due to the 1D electrode $[(Ge_5)Fe]_\infty$ having the fivefold axis of symmetry (along the z axis), we only consider the cases where the tilting angles vary from 0° to 72° at intervals of 9°. Our calculation demonstrated that the orientations of BDT have some effect on the MR and SIE values, but the effect is not very significant (see Fig. 5). The results show clearly that our proposed molecular junction is robust against the BDT orientations.

In summary, we have investigated the spin-polarized transport in the $[(Ge_5)Fe]_\infty$-BDT-$[(Ge_5)Fe]_\infty$ magnetic molecular junction using the NEGF-DFT method. We found that this structure not only contains an extremely large magnetoresistance ratio but also has perfect spin injection effects for PC. These remarkable spin transport properties are not sensitive to the tilting angles formed by the BDT molecular plane and the yz plane. The results show that the $[(Ge_5)Fe]_\infty$-BDT-$[(Ge_5)Fe]_\infty$ device should be a promising candidate for future molecular spintronics devices.

This work was supported by the National Natural Science Foundation of China (Grant Nos. 11504072 and 11404273).

[1]T. Miyazaki and N. Tezuka, J. Magn. Magn. Mater. **139**, L231–L234 (1995).
[2]Z. Wen, H. Sukegawa, S. Mitani, and K. Inomata, Appl. Phys. Lett. **98**, 192505 (2011).
[3]W. Wulfhekel, M. Klaua, D. Ullmann, F. Zavaliche, J. Kirschner, R. Urban, T. Monchesky, and B. Heinrich, Appl. Phys. Lett. **78**, 509 (2001).

[4]S. Ikeda, J. Hayakawa, Y. Ashizawa, Y. M. Lee, K. Miura, H. Hasegawa, M. Tsunoda, F. Matsukura, and H. Ohno, Appl. Phys. Lett. **93**, 082508 (2008).
[5]N. Tezuka, N. Ikeda, F. Mitsuhashi, and S. Sugimoto, Appl. Phys. Lett. **94**, 162504 (2009).
[6]Y. Ohdaira, M. Oogane, H. Naganuma, and Y. Ando, Appl. Phys. Lett. **99**, 132513 (2011).
[7]L. Bogani and W. Wernsdorfer, Nat. Mater. **7**, 179–186 (2008).
[8]A. R. Rocha, V. M. García-suárez, S. W. Bailey, C. J. Lambert, J. Ferrer, and S. Sanvito, Nat. Mater. **4**, 335–339 (2005).
[9]C. H. Hsu, Y. H. Chu, C. I. Lu, P. J. Hsu, S. W. Chen, W. J. Hsueh, C. C. Kaun, and M. T. Lin, J. Phys. Chem. C **119**, 3374–3378 (2015).
[10]J. Zeng and K. Q. Chen, J. Mater. Chem. C **1**, 4014 (2013).
[11]D. Waldron, P. Haney, B. Larade, A. MacDonald, and H. Guo, Phys. Rev. Lett. **96**, 166804 (2006).
[12]B. B. Zhou, M. S. Denning, D. L. Kays, and J. M. Goicoechea, J. Am. Chem. Soc. **131**, 2802 (2009).
[13]X. Li, Y. Ma, Y. Dai, and B. Huang, J. Mater. Chem. C **1**, 4565 (2013).
[14]H. Ebert, P. Strange, and B. L. Gyorffy, J. Phys. F: Met. Phys. **18**, L135–Ll39 (1988).
[15]J. Taylor, H. Guo, and J. Wang, Phys. Rev. B **63**, 245407 (2001).
[16]G. Kresse and J. Furthmuller, Phys. Rev. B **54**, 11169 (1996).
[17]J. Junquera, Ó. Paz, D. Sánchez-Portal, and E. Artacho, Phys. Rev. B **64**, 235111 (2001).
[18]Y. Meir and N. S. Wingreen, Phys. Rev. Lett. **68**, 2512 (1992).
[19]A. P. Jauho, N. S. Wingreen, and Y. Meir, Phys. Rev. B **50**, 5528 (1994).
[20]S. S. P. Parkin, C. Kaiser, A. Panchula, P. M. Rice, B. Hughes, M. Samant, and S. H. Yang, Nat. Mater. **3**, 862 (2004).
[21]S. Yuasa, T. Nagahama, A. Fukushima, Y. Suzuki, and K. Ando, Nat. Mater. **3**, 868 (2004).
[22]R. Pati, L. Senapati, P. M. Ajayan, and S. K. Nayak, Phys. Rev. B **68**, 100407 (2003).
[23]A. R. Rocha, V. M. Garcia-Suarez, S. Bailey, C. Lambert, J. Ferrer, and S. Sanvito, Phys. Rev. B **73**, 085414 (2006).
[24]R. Yamada, M. Noguchi, and H. Tada, Appl. Phys. Lett. **98**, 053110 (2011).
[25]K. Horiguchi, T. Sagisaka, S. Kurokawa, and A. Sakai, J. Appl. Phys. **113**, 144313 (2013).
[26]J. S. Moodera, J. Nowak, and R. J. M. van de Veerdonk, Phys. Rev. Lett. **80**, 2941 (1998).
[27]S. Sen and S. Chakrabarti, J. Am. Chem. Soc. **132**, 15334–15339 (2010).